Analyst

PAPER

View Article Online
View Journal | View Issue

Cite this: *Analyst*, 2019, **144**, 691

A rolling circle amplification-assisted DNA walker triggered by multiple DNAzyme cores for highly sensitive electrochemical biosensing

Sina Wang, Yuhang Ji, Haomin Fu, Huangxian Ju and Jianping Lei *

DNA walkers from monopodial to multipedal types have usually one cleavage site to power the walking system along with the track. Herein, a multipedal DNA walker (m-DNA walker) with multiple DNAzyme cores was constructed with the assistance of rolling circle amplification (RCA) for highly sensitive electrochemical biosensing. Firstly, a three-component DNA complex as a swing strand was prepared by integrating a padlock, an RCA primer and a block DNA as a recognition element in the DNA walker system. After ferrocene-labeled track DNA (trDNA) and capture DNA were fixed on a gold electrode, the three-component DNA complex was imported onto the electrode as a swing arm to form a m-DNA walker. In the presence of target DNA and a RCA kit, the block was displaced from the complex and RCA was initiated to form multiple DNAzyme strands. Upon hybridization with trDNA, the m-DNA walker was motivated by the cleavage of multiple DNAzyme cores in the presence of manganese ions to free signal molecules. Under the optimal circumstances, the electrochemical m-DNA walker showed a linear range from 1.0 fM to 1.0 nM with a detection limit of 0.28 fM. Moreover, the m-DNA walker demonstrated a rapid cleavage rate and a low ratio of the swing strand to the track, which is more excellent than a single foot walker and a bipedal DNA walker. The practicality of the proposed strategy was also confirmed by detecting target DNA in 10% human serum, showing promising applications in clinical diagnosis.

Received 3rd October 2018,
Accepted 13th November 2018

DOI: 10.1039/c8an01892h

rsc.li/analyst

Introduction

With the development of DNA nanotechnology, DNA walkers can accurately perform all kinds of transport functions and signal transduction with high chemical yield and speed.[1] Currently, multifarious DNA walkers have been extensively investigated for biosensing,[2–4] "cargo" transportation[5,6] and organic synthesis.[7] According to the number of feet, DNA walkers are divided into three categories, including monopodial,[8,9] bipedal[10,11] and multipedal[12] walking devices. A series of single foot DNA walkers (s-DNA walker) powered by nicking endonucleases and DNAzymes were designed *via* the self-assembly of a swing strand on gold nanoparticles for nucleic acid analysis.[13,14] Considering that the s-DNA walker was confined in a certain region, a bipedal or multipedal DNA walker was sequentially developed by a toehold-mediated strand displacement reaction, which can move along the track for the enhancement of signal transduction.[15,16] Nevertheless, the bipedal or multipedal walkers might be easier to dissociate from the footpath compared with binding monopodial walkers. Therefore, it is significant to design a single swing strand containing multiple binding sites which not only prevents the dissociation from the track but also generates multiple DNAzymes to accelerate signal amplification.

DNA walkers can move processively and autonomously along various man-made tracks containing double stranded DNA,[17] DNA origami,[18,19] DNA monolayers,[20] nanoparticles or microparticles.[21] The walking process is fueled by the toehold-mediated strand displacement reaction,[22,23] DNAzyme-mediated DNA hydrolysis,[24,25] nicking enzymes[26,27] and environmental stimuli.[28,29] Different from the DNA sequences as swing strands in the s-DNA walker or the bipedal DNA walker (b-DNA walker), the ingredients of swing strands in the m-DNA walker are more abundant. For example, a streptavidin molecule was involved in the DNA walker as an insert "body" and moved along the origami track with 50 cleavage steps.[30] A "sandwich biscuit" m-DNA walker was proposed based on two DNA-modified gold nanocrystals crosslinking two origami filaments to accomplish sliding in opposite directions.[31] Here, a m-DNA walker was designed with the assistance of rolling circle amplification (RCA) to generate multiple DNAzyme cores in a single swing strand for signal transduction.

State Key Laboratory of Analytical Chemistry for Life Science, School of Chemistry and Chemical Engineering, Nanjing University, Nanjing 210023, China.
E-mail: jpl@nju.edu.cn

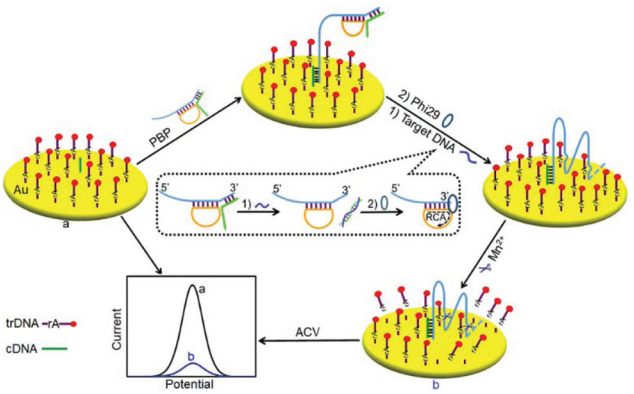

Scheme 1 Schematic diagram of the construction of the RCA-assisted DNA walker with multiple DNAzyme cores for electrochemical biosensing.

RCA as a specific isothermal enzymatic procedure driven by DNA polymerase can duplicate circularized oligonucleotide templates along the DNA primer with either linear or geometric kinetics with high efficiency and speed.[32–36] In this work, coupling with RCA, we developed a m-DNA walker with a prolonged strand as multiple DNAzyme cores to trigger the walking for signal amplification (Scheme 1). Firstly, ferrocene (Fc)-labeled track DNA (trDNA) and capture DNA (cDNA) at a certain ratio were assembled on the gold electrode. Then the as-prepared electrode was incubated with the padlock/block/primer (PBP) complex to form the DNA walker. Upon adding the target DNA and the RCA kit, the block of the PBP was replaced and the RCA was triggered to generate the RCA product involving many sections partially complementary to trDNA. Subsequently, multiple DNAzyme cores were generated in the presence of Mn^{2+}, and thus could cleave the hybridized trDNA, resulting in the detachment of the ferrocene molecules from the electrode surface and the liberty of the swing arms. The free swing arms would hybridize with trDNA to duplicate the cleavage process; as a result, a large change of the electrochemical current was obtained for signal amplification. Hence, a convincing strategy was developed to detect target DNA with excellent performance such as a low detection limit and high specificity, suggesting its potential application in biosensing. The DNA walker with multiple DNAzyme cores not only avoids the dissociation of walking strands from the track, but also provides a new avenue for signal transduction in biosensing.

Experimental

Materials and reagents

Tris(2-carboxyethyl) phosphine hydrochloride (TCEP), 6-mercaptohexanol (MCH) and hexaammineruthenium(III) chloride (RuHex) were obtained from Sigma-Aldrich (St Louis, MO, USA). Phi29 DNA polymerase (Phi29), dNTPs and RCA reaction buffer were bought from New England Biolabs Ltd. Oligonucleotide sequences and tris(hydroxymethyl)aminomethane (Tris) were purchased from Sangon Bioengineering Co., Ltd (Shanghai, China), except the circular padlock DNA which was received from TaKaRa Biotechnology Co. Ltd (Dalian, China). All these reagents were used without further purification and ultrapure water (18 MΩ cm^{-1}, Milli-Q, Millipore) was used in the whole assay. Healthy serum samples were generously provided by Jiangsu Province Tumor Hospital. The DNA was dissolved in 25 mM Tris-HCl buffer containing 200 mM NaCl (pH 7.4), and its sequences are listed as follows from the 5′ end to the 3′ end:

trDNA: HS-TTTTTTTTTTACTATrAGGAAGAG-Fc

non-cleavage trDNA: HS-TTTTTTTTTTACTATAGGAAGAG-Fc

cDNA: CTCTCTCTACCCACGTTTTTTTTTT-SH

Primer: TTTTTCGTGGGTAGAGAGAG$(T)_{20}$GGTTGCAGTCTC-TTCTTTTTAGAACCGAATTTGTG

Padlock: ACTATTTCGACCGGCTCGGAGAAGAGACTGCAACC-ATCAGTCAGTC

Target: TACCCTGTAGAACCGAATTTGTG

Block: AAGAGACACAAATTCGGTTCTACAGGGTA

Swing 1 (S1): TTTTTCGTGGGTAGAGAGAG$(T)_{57}$AGAACCGA-ATTTGTGTCTCTTCTCCGAGCCGGTCGAAATAGT

Swing 2 (S2): TTTTTCGTGGGTAGAGAGAG$(T)_{15}$AGAACCG-AATTTGTGTCTCTTCTCCGAGCCGGTCGAAATAGTAGAACCGA-ATTTGTGTCTCTTCTCCGAGCCGGTCGAAATAGT

The PBP complex obtained from the mixture of the padlock (1.0 μM), the primer (1.0 μM) and the block (1.5 μM) was annealed at 95 °C for 5 min, and then slowly cooled down to 25 °C.

Fabrication of the m-DNA walker

Firstly, the gold electrode was immersed in a freshly prepared piranha solution (H_2SO_4/30% H_2O_2, 3 : 1) for 60 min, in order to eliminate any organic matter from the gold surface. Then, the gold electrode was carefully polished with 0.05 μm α-Al_2O_3 slurry to achieve a mirror-like surface, and electrochemically activated in a 1.0 M H_2SO_4 solution. Afterward, it was thoroughly rinsed with ultrapure water and dried with soft nitrogen.

Secondly, 10 μL of trDNA (10 μM) and 1.0 μL of cDNA (1.0 μM) were mixed with 5.0 μL of TCEP (10 mM) for 1.0 h to reduce disulfide bonds, following a dilution with 25 mM Tris-HCl buffer containing 200 mM NaCl (pH 7.4) to a total volume of 100 μL, and thus a mixture of 1.0 μM trDNA and 0.01 μM cDNA was obtained. An amount of 5.0 μL of the above solution was dropped on the electrode surface, and incubated at 37 °C for 2 h. After rinsing with 10 mM phosphate buffer (PBS) and drying with nitrogen, 5.0 μL of 1.0 mM MCH was dropped on the electrode for 1.0 h at 37 °C to seal the unmodified sites. After washing with PBS to remove redundant MCH and DNA, the electrode was incubated with 5.0 μL of the mixture of the primer, the block and the padlock involving a PBP complex at 37 °C for 120 min, and a binding m-DNA walker was obtained. Similarly, the s-DNA walker containing a single DNAzyme core and the b-DNA walker containing two DNAzyme cores were established by the hybridization of blocked swing 1 and swing 2 with cDNA on the trDNA and cDNA co-modified electrodes, respectively. The non-DNA walker was fabricated on the non-cleaved trDNA and cDNA co-modified electrodes. Finally, these

constructed DNA walkers were rinsed with PBS, dried with nitrogen and stored at 4 °C before use.

Procedure for the preparation of RCA assisted-DNA walker

The RCA reaction mixture was first prepared by mixing 5.0 μL of 10× RCA reaction buffer, 8.0 μL of dNTPs (2.5 mM each of dATP, dCTP, dGTP and dTTP), 1.0 μL of Phi29 DNA polymerase stock (10 U μL^{-1}), 2.5 μL of the target (a certain concentration), 1.25 μL of Mn^{2+} (20 mM) and 32.25 μL of water. Then, the m-DNA walker was initiated by incubating with the RCA reaction mixture at 37 °C for 1.0 h. Consequently, the biosensor was subjected to electrochemical measurements after washing with 10 mM PBS (pH 7.4).

Gel electrophoresis analysis

15% native polyacrylamide gel was prepared using 1 × TBE buffer. The loading sample was prepared by mixing 7.0 μL DNA sample with 1.5 μL of 6 × loading buffer, and then 5.0 μL of the mixture was injected into the polyacrylamide gel. The gel electrophoresis was performed at 90 V for 45 min in 1 × TBE buffer and staining was done with GelRed dye for 30 min. Finally, the resulting bands were observed with a Molecular Imager Gel Doc XR. On the other hand, in order to identify the product of RCA at different times, a 0.6% agarose gel was prepared using 1 × TBE buffer and 1 × GelRed dye. The agarose gel electrophoresis was performed by loading the samples containing the RCA product and 6 × loading buffer in the hydrogel, run at 100 V for 90 min in 1 × TBE buffer and visualized *via* a Molecular Imager Gel Doc XR.

Electrochemical measurements

All electrochemical experiments were performed on a CHI 660D electrochemical workstation (Shanghai CH Instruments, China) with the m-DNA walker substrate as the working electrode (2.0 mm in diameter), a platinum wire as the counter electrode, and a saturated calomel electrode as the reference. These three electrodes were immersed in 10 mM PBS (pH 7.4) containing 0.1 M $NaClO_4$ and electrochemically tested using alternating current voltammetry (ACV, the detection range from 0 to +0.6 V, at a frequency of 25 Hz and with an amplitude of 25 mV, a step potential of 4 mV). Chronocoulometry (CC) measurements were performed at a sample interval of 0.25 ms and a pulse width of 0.5 s in 10 mM PBS containing 50 μM RuHex.

Results and discussion

Design and detection principle

The RCA-assisted DNA walker with multiple DNAzyme cores was constructed for sensitive electrochemical DNA detection (Scheme 1). Fc-labeled trDNA was self-assembled on the gold electrode through Au–thiol bonds as both track and signal molecules, along with a portion of cDNA. The trDNA is a DNA–RNA jogged sequence consisting of an RNA nucleotide flanked by two DNA regions, which are the binding zones of two arms of the DNAzyme. Meanwhile, a three-component DNA complex was made up of a primer, a block and a padlock, complementary to the DNAzyme sequence. In the absence of the target DNA, the primer/block duplex prevents Phi29 from performing 3′–5′ digestion of the "primer", indicating a "close" state.[37] The presence of target DNA, however, triggers the release of the block from the PBP complex, exposing the 3′ element of the "primer" for nucleolytic clipping. This in turn converted the "primer" into a mature primer to enable RCA, and produced multiple DNAzyme cores on the primer chain. Sequentially, in the presence of Mn^{2+}, the formed Mn^{2+} DNAzyme cleaved the trDNA molecule, releasing the Fc-labeled fragment. The fracture of the chimeric DNA–RNA supplied the fuel for the DNAzyme to achieve autonomous movement along the electrode surface. As a result, a large amount of Fc-labeled fragments of the trDNA were released for signal amplification, and thus a highly sensitive method was developed for the electrochemical detection of the target DNA.

Feasibility of the m-DNA walker

The feasibility of the biosensor was determined by performing ACV in different solutions (Fig. 1A). When the m-DNA walker was incubated with Tris-HCl buffer, an obvious oxidation peak of Fc was observed (curve a). Upon adding the mixture of the RCA kit, the target DNA and Mn^{2+}, the electrochemical signal fell sharply down to 14% owing to the stepwise cutting of the m-DNA walker (curve b). As a comparison, the DNA walkers with a single-core DNAzyme (s-DNA walker) and two DNAzyme cores (b-DNA walker) were treated with a mixture of target DNA and Mn^{2+}. As shown in Fig. 1A, the remaining electrochemical signals of the s-DNA walker and the b-DNA walker are 4.4-fold (curve c) and 3.1-fold (curve d) that of the m-DNA walker, respectively. Besides, the non-DNA walker shows no obvious response to the target (curve e). These results indicated that the m-DNA walker can provide a lower background, leading to a sensitive approach for electrochemical detection.

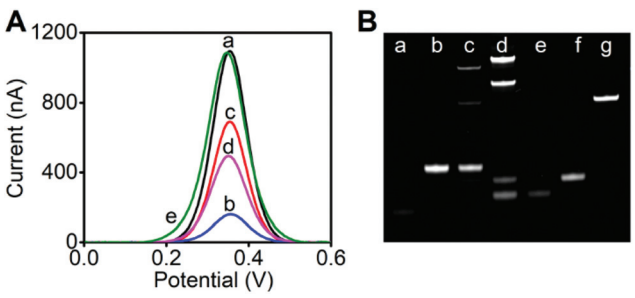

Fig. 1 (A) ACV responses of the m-DNA walker before (a) and after (b) incubating with 0.5 nM target + RCA kit + 0.5 mM Mn^{2+} in Tris-HCl buffer, s-DNA walker (c), b-DNA walker (d), and non-DNA walker (e) incubated with 0.5 nM target + 0.5 mM Mn^{2+}. (B) Polyacrylamide gel of the target (lane a), a mixture of the block and target DNA at a 1 : 1 molar ratio (lane b), the target DNA + PBP complex (lane c), a mixture of the primer, the padlock and the block at a 1 : 1 : 1.5 molar ratio (lane d), the block (lane e), the padlock (lane f), and the primer (lane g).

Polyacrylamide gel electrophoresis (PAGE) was then used to test the strand displacement between the PBP complex and the target DNA (Fig. 1B). Comparing with individual lanes for the target DNA (lane a) and the block (lane e), only one lane appeared after mixing the target DNA and the block, indicating the formation of a duplex of the target DNA/block (lane b). When adding the target DNA to the PBP complex (lane d) prepared by mixing the primer (lane g), the padlock (lane f) and the block, a band of the PBP complex disappeared while a band corresponding to the duplex of the target/block appeared (lane c). Moreover, the displacement product was obtained with a slow immigration rate in lane c, which could correspond to the padlock/primer duplex for the sequential RCA process.

The density of DNA fixed on the gold electrode was calculated by CC measurements using RuHex as a redox marker (Fig. 2A). On the basis of the Cottrell equation and Faraday's law,[38,39] the density of DNA was approximately 1.32×10^{12} molecules per cm^2 corresponding to 8.7 nm of an intermolecular spacing, which is beneficial to the reaction between trDNA and DNAzyme. Considering the size of trDNA (about 8.5 nm), the length of the padlock (15.6 nm) is sufficient to reach the adjacent trDNA for the next cleavage.

Electrochemical impedance spectroscopy (EIS) was investigated to characterize each step of the experimental process (Fig. 2B). The bare gold electrode showed a relatively small electron transfer resistance (R_{et}) (curve a). After modification with trDNA and cDNA, R_{et} shows a tremendous increase (curve b) because the negatively charged DNA monolayer repelled $[Fe(CN)_6]^{3-/4-}$ from the electrode surface, suggesting that the trDNA and cDNA were successfully immobilized on the electrode. The incubation of trDNA and the cDNA co-modified gold electrode with PBP further increased the R_{et} (curve c) due to the large steric effect of the PBP complex.[20] Nevertheless, upon the addition of Mn^{2+}, the R_{et} was greatly reduced through the extensive cleavage of trDNA (curve d). These results demonstrated that the m-DNA walker was highly efficient for signal transduction.

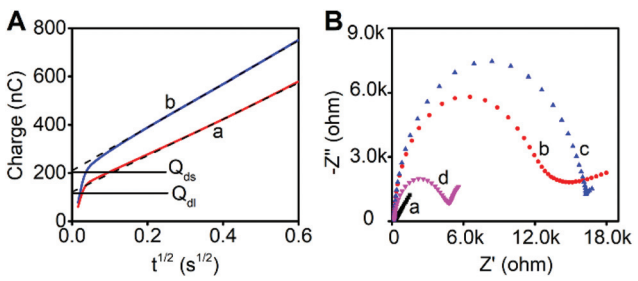

Fig. 2 (A) CC curves at the MCH-modified electrode (a) and trDNA and cDNA co-modified electrodes (b) in 10 mM PBS containing 50 μM RuHex. The intercept ($t^{1/2} = 0$) represents the charge of RuHex adsorbed at the electrode surface. Q_{dl} and Q_{ds} are the capacitive charge and the total charge of capacitive and adsorbed reactant charge, respectively. (B) EIS of bare electrode (a) and trDNA and cDNA co-modified electrodes (b); (c) and (d) are m-DNA walkers before and after incubation with 0.5 nM target, RCA kit and 0.5 mM Mn^{2+}, respectively.

Optimization of conditions

To realize the excellent performance of the m-DNA walker, several crucial experimental parameters were optimized, including the fixed time, the cleavage time and the ratio of trDNA to cDNA concentrations. The density of DNA fixed on the gold electrode was related to the immobilization time, and the ACV response reached a plateau after incubating with trDNA and cDNA for 120 min due to the limited binding sites (Fig. 3A). The flexibility of the swing strand was of vital importance for trDNA hybridization; we assessed that the product of RCA varied with the reaction time (Fig. 3B). The base numbers of the RCA product were mostly distributed from 2500 bp to 15 000 bp, corresponding to 52-cycles and 324-cycles of the padlock. Considering the distance of adjacent trDNAs, two DNAzyme cores in the m-DNA walker could approach one trDNA. Therefore, one DNAzyme swing strand can approximately increase trDNA molecules from 2.8×10^3 to 1.1×10^5, indicating the capacity of the m-DNA walker for signal amplification.

Advantages of the m-DNA walker

Additionally, the cleavage time of the DNAzyme was optimized (Fig. 4A). When the s-DNA walker was incubated with a mixture of the target DNA and Mn^{2+}, the ACV signal reached a steady state at 120 min (curve a). After the RCA kit, the target

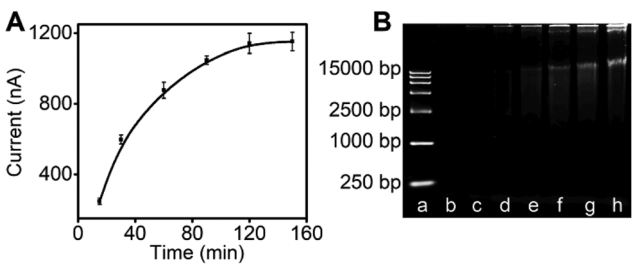

Fig. 3 (A) Effect of the immobilization time of trDNA and cDNA on the ACV response. (B) Agarose gel electrophoresis image of the RCA product for PBP in the presence of the target DNA at 5, 15, 30, 60, 90, 120, and 180 min (from lanes b to h). Lane a is the DNA marker.

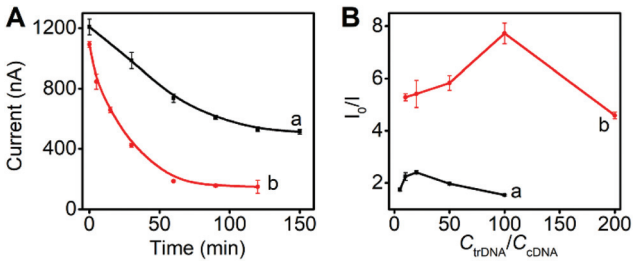

Fig. 4 (A) Effects of the cleavage time of the Mn^{2+} DNAzyme for the s-DNA walker (a) and the m-DNA walker (b) on the ACV response in the presence of 0.5 nM target and 0.5 mM Mn^{2+}. (B) Effects of the concentration ratio of trDNA to cDNA for the construction of the s-DNA walker (a) and the m-DNA walker (b) on the ACV response. I and I_0 represent the current signal with and without target DNA, respectively.

DNA and Mn^{2+} were added to the m-DNA walker and the peak current signal decreased as the reaction time increased, until it reached a platform at 60 min (curve b). Hence, 60 min was chosen as the perfect RCA reaction time and cleavage time, which was also identified from the agarose gel electrophoresis image of the RCA product. In a word, the m-DNA walker has a more efficient cleavage rate compared to the s-DNA walker.

Another key condition is the concentration ratio of trDNA to cDNA. As shown in Fig. 4B, the values of I_0/I first increased to 2.4 and 7.8 at the ratios of trDNA to cDNA of 20 and 100 for the s-DNA walker (curve a) and the m-DNA walker (curve b), respectively, and then changed oppositely at the high ratio of trDNA to cDNA. This phenomenon could be explained based on the fact that the low ratio of trDNA to cDNA might lead to the overlap of trDNAs with each other, and a much higher ratio of trDNA to cDNA caused the incomplete cleavage. Consequently, comparing with the s-DNA walker, the m-DNA walker showed a higher ratio of trDNA to cDNA, that is, we employ fewer "swing strand" but accomplish more cleavages, which shows the superiority of our strategy.

Assay performance

At the optimized experimental parameters, we further analyzed the biosensor in response to various concentrations of the target DNA by ACV measurements. As expected, the peak current steadily declined with the increase of the target DNA concentration in the range of 1.0 fM to 1.0 nM (Fig. 5A). A linear relationship was observed between the peak current (I) and the logarithm of the target concentration with the linear regression equation of I (nA) = $-150.2 \log C_{\text{Target}}$ (nM) + 146.6 (Fig. 5B, line b). The detection limit was calculated to be 0.28 fM, benefiting from the superior performance of RCA-assisted DNA walker cleavage triggered by multiple DNAzyme cores. It is much lower than 500 fM of a recyclable biointerface based on cross-linked branched DNA nanostructures,[40] 1.0 fM of an electrical double layer gated high electron mobility transistor,[41] and 10 fM of a localized surface plasmon resonance-coupled fiber-optic nanoprobe.[42] In contrast, the s-DNA walker (Fig. 5B, line a) is less sensitive than the m-DNA walker based on multiple DNAzyme cores, which further proves the advantage of our strategy. The reproducibility was measured by detecting a 10 pM target with six biosensors. The relative standard deviation (RSD) of the six repeated tests was 3.1%, which implied that the proposed electrochemical biosensor has good reproducibility. In addition, the stability of the biosensor was challenged by storing it at 4 °C for 10 days; it retained 92.9% of its initial current, indicating tolerable stability.

The metal cofactors are usually required to achieve the catalytic activity of the DNAzyme.[13] We tested the m-DNA walker in response to 0.5 nM target DNA and different divalent metal ions. The effect of multiple DNAzyme-core cleavage processes follows the order of $Mn^{2+} > Zn^{2+} > Mg^{2+} > Pb^{2+} > Ca^{2+}$ (Fig. 5C), showing the specific response of the Mn–DNAzyme to Mn^{2+}. We examined the specificity of the biosensor by testing several DNA sequences (Fig. 5D). The decrease of the current resulting from the 0.5 nM target sequence is significantly larger than

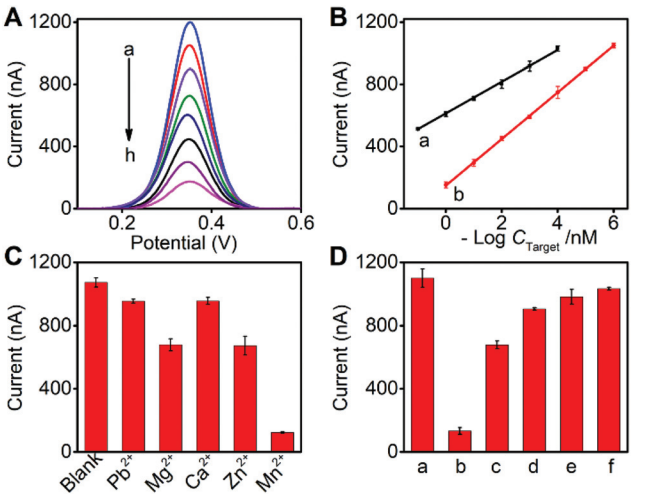

Fig. 5 (A) ACV responses of the m-DNA walker to 0, 0.001, 0.01, 0.1, 1.0, 10.0, 100.0, and 1000 pM target under optimal conditions (from a to h). (B) Plot of the peak current *vs.* logarithm of the target concentration for the s-DNA walker (a) and the m-DNA walker (b). Error bars represent the standard deviations of three parallel experiments. (C) The ACV responses of the m-DNA walker tested using 0.5 nM target DNA and different divalent metal ions as cofactors. The concentrations of metal ions were 0.5 mM Mn^{2+}, 10 mM Mg^{2+}, 10 mM Ca^{2+}, 0.01 mM Zn^{2+}, and 0.2 mM Pb^{2+}. (D) Specificity of the m-DNA walker in response to Tris-HCl buffer (a), 0.5 nM target DNA (b), single-base mismatched DNA (c), two-base mismatched DNA (d), three-base mismatched DNA (e), and random DNA (f).

those from the four variants at the same concentration, suggesting that the m-DNA walker can effectively differentiate the complementary target from these mismatched strands.

Also, recovery tests were performed to examine the practicability of the m-DNA walker for detecting target DNA in a physiological environment. Three different concentrations of the target were scattered in 10-fold diluted healthy serum as samples. The recovery of the target ranged from 97.9% to 103.6%, and the RSDs were between 3.7% and 8.0%. These results showed that the fabricated biosensor had a promising application in the detection of DNA in clinical diagnosis.

Conclusions

In this work, a RCA-assisted DNA walker with multiple DNAzyme cores was successfully constructed for sensitive and selective electrochemical biosensing. We designed a three-component DNA complex as a swing strand, the RCA primer and a recognition element to target in the DNA walker system. With the assistance of the target DNA and a RCA kit, the swing strand can be extensively expanded up to 324-cycles of the padlock, and thus the m-DNA walker with multiple DNAzyme cores was formed to obtain a high turnover for signal amplification. Comparing with the s-DNA walker or the b-DNA walker, the m-DNA walker showed 4.4- and 3.1-fold lower background, leading to a much lower detection limit. Therefore, the m-DNA

walker allows a detection limit down to the sub-ficomolar level with the linear range up to six orders of magnitude. What's more, the m-DNA walker protocol not only demonstrated the rapid cleavage rate and a low ratio of the swing strand to the track but also avoided the dissociation of the walking strands from the track due to the binding swing strand. To the best of our knowledge, this is the first report on the DNA walker with multiple DNAzyme cores, and opens up a new direction for signal amplification in biosensing.

Conflicts of interest

There are no conflicts to declare.

Acknowledgements

We gratefully acknowledge the National Natural Science Foundation of China (21675084 and 21635005), and National Key Technologies R&D Program (2016YFC0302500).

Notes and references

1 X. M. Qu, D. Zhu, G. B. Yao, S. Su, J. Chao, H. J. Liu, X. L. Zuo, L. H. Wang, J. Y. Shi, L. H. Wang, W. Huang, H. Pei and C. H. Fan, *Angew. Chem., Int. Ed.*, 2017, **56**, 1855–1858.
2 C. Li, X. X. Li, L. M. Wei, M. Y. Liu, Y. Y. Chen and G. X. Li, *Chem. Sci.*, 2015, **6**, 4311–4317.
3 W. Li, L. Wang and W. Jiang, *Chem. Commun.*, 2017, **53**, 5527–5530.
4 F. Tao, J. Fang, Y. C. Guo, Y. Y. Tao, X. L. Han, Y. X. Hu, J. J. Wang, L. Y. Li, Y. L. Jian and G. M. Xie, *Anal. Biochem.*, 2018, **554**, 16–22.
5 E. Del Grosso, A. Amodio, G. Ragazzon, L. J. Prins and F. Ricci, *Angew. Chem., Int. Ed.*, 2018, **57**, 10489–10493.
6 H. Z. Gu, J. Chao, S. J. Xiao and N. C. Seeman, *Nature*, 2010, **465**, 202–205.
7 Y. He and D. R. Liu, *Nat. Nanotechnol.*, 2010, **5**, 778–782.
8 M. Q. He, K. Wang, W. J. Wang, Y. L. Yu and J. H. Wang, *Anal. Chem.*, 2017, **89**, 9292–9298.
9 C. Jung, P. B. Allen and A. D. Ellington, *ACS Nano*, 2017, **11**, 8047–8054.
10 T. E. Tomov, R. Tsukanov, Y. Glick, Y. Berger, M. Liber, D. Avrahami, D. Gerber and E. Nir, *ACS Nano*, 2017, **11**, 4002–4008.
11 K. Wang, M. Feng, M. Q. He, F. H. Zhai, Y. Dai, R. H. He and Y. L. Yu, *Talanta*, 2018, **188**, 685–690.
12 C. Jung, P. B. Allen and A. D. Ellington, *Nat. Nanotechnol.*, 2016, **11**, 157–163.
13 H. Y. Peng, X. F. Li, H. Q. Zhang and X. C. Le, *Nat. Commun.*, 2017, **8**, 14378–14390.
14 X. L. Yang, Y. A. Tang, S. D. Mason, J. B. Chen and F. Li, *ACS Nano*, 2016, **10**, 2324–2330.
15 N. X. Li, M. Y. Du, Y. C. Liu, X. H. Ji and Z. K. He, *ACS Sens.*, 2018, **3**, 1283–1290.
16 J. Zhang, L. L. Wang, M. F. Hou, Y. K. Xia, W. H. He, A. Yan, Y. P. Weng, L. P. Zeng and J. H. Chen, *Biosens. Bioelectron.*, 2018, **102**, 33–40.
17 Y. Chen, Y. Xiang, R. Yuan and Y. Q. Chai, *Nanoscale*, 2015, **7**, 981–986.
18 M. Teichmann, E. Kopperger and F. C. Simmel, *ACS Nano*, 2014, **8**, 8487–8496.
19 D. F. Wang, C. Vietz, T. Schröder, G. Acuna, B. Lalkens and P. Tinnefeld, *Nano Lett.*, 2017, **17**, 5368–5374.
20 J. Zhu, H. Y. Gan, J. Wu and H. X. Ju, *Anal. Chem.*, 2018, **90**, 5503–5508.
21 C. Feng, Z. H. Wang, T. S. Chen, X. X. Chen, D. S. Mao, J. Zhao and G. X. Li, *Anal. Chem.*, 2018, **90**, 2810–2815.
22 L. D. Wang, R. J. Deng and J. H. Li, *Chem. Sci.*, 2015, **6**, 6777–6782.
23 S. Z. Lv, K. Y. Zhang, Y. Y. Zeng and D. P. Tang, *Anal. Chem.*, 2018, **90**, 7086–7093.
24 S. X. Cai, M. Chen, M. M. Liu, W. H. He, Z. J. Liu, D. Z. Wu, Y. K. Xia, H. H. Yang and J. H. Chen, *Biosens. Bioelectron.*, 2016, **85**, 184–189.
25 K. Wang, M. Q. He, F. H. Zhai, J. Wang, R. H. He and Y. L. Yu, *Biosens. Bioelectron.*, 2018, **105**, 159–165.
26 Y. H. Ji, L. Zhang, L. Y. Zhu, J. P. Lei, J. Wu and H. X. Ju, *Biosens. Bioelectron.*, 2017, **96**, 201–205.
27 K. Yehl, A. Mugler, S. Vivek, Y. Liu, Y. Zhang, M. Z. Fan, E. R. Weeks and K. Salaita, *Nat. Nanotechnol.*, 2016, **11**, 184–190.
28 Y. Y. Yang, M. A. Goetzfried, K. Hidaka, M. X. You, W. H. Tan, H. Sugiyama and M. Endo, *Nano Lett.*, 2015, **15**, 6672–6676.
29 M. X. You, Y. Chen, X. B. Zhang, H. P. Liu, R. W. Wang, K. L. Wang, K. R. Williams and W. H. Tan, *Angew. Chem., Int. Ed.*, 2012, **51**, 2457–2460.
30 K. Lund, A. J. Manzo, N. Dabby, N. Michelotti, A. Johnson-Buck, J. Nangreave, S. Taylor, R. J. Pei, M. N. Stojanovic, N. G. Walter, E. Winfree and H. Yan, *Nature*, 2010, **465**, 206–210.
31 M. J. Urban, S. Both, C. Zhou, A. Kuzyk, K. Lindfors, T. Weiss and N. Liu, *Nat. Commun.*, 2018, **9**, 1454–1460.
32 J. Ma, L. Wu, Z. H. Li, Z. C. Lu, W. M. Yin, A. X. Nie, F. Ding, B. R. Wang and H. Y. Han, *Anal. Chem.*, 2018, **90**, 7415–7421.
33 W. T. Yang, Y. Shen, D. Y. Zhang and W. J. Xu, *Chem. Commun.*, 2018, **54**, 10195–10198.
34 Q. Li, F. P. Zeng, N. Lyu and J. Liang, *Analyst*, 2018, **143**, 2304–2309.
35 K. Y. Zhang, S. Z. Lv, Z. Z. Lin, M. J. Li and D. P. Tang, *Biosens. Bioelectron.*, 2018, **101**, 159–166.
36 K. Y. Zhang, S. Z. Lv, M. H. Lu and D. P. Tang, *Biosens. Bioelectron.*, 2018, **117**, 590–596.
37 M. Liu, Q. Zhang, D. R. Chang, J. Gu, J. D. Brennan and Y. F. Li, *Angew. Chem., Int. Ed.*, 2017, **56**, 6142–6146.

38 A. B. Steel, T. M. Herne and M. J. Tarlov, *Anal. Chem.*, 1998, **70**, 4670–4677.
39 B. Yao, Y. C. Liu, M. Tabata, H. T. Z. Zhu and Y. Miyahara, *Chem. Commun.*, 2014, **50**, 9704–9706.
40 F. Li, Y. H. Dong, Z. K. Zhang, M. Lv, Z. Wang, X. H. Ruan and D. Y. Yang, *Biosens. Bioelectron.*, 2018, **117**, 562–566.
41 Y. W. Chen, T. Y. Tai, C. P. Hsu, I. Sarangadharan, A. K. Pulikkathodi, H. L. Wang, R. Sukesan, G. Y. Lee, J. I. Chyi, C. C. Chen, G. B. Lee and Y. L. Wang, *Sens. Actuators, B*, 2018, **271**, 110–117.
42 S. Kaye, Z. Zeng, M. Sanders, K. Chittur, P. M. Koelle, R. Lindquist, U. Manne, Y. B. Lin and J. J. Wei, *Analyst*, 2017, **142**, 1974–1981.